X-ray Standing Waves and Surface EXAFS Studies of Electrochemical Interfaces

H. D. ABRUÑA,* G. M. BOMMARITO,† AND H. S. YEE‡

Department of Chemistry, Baker Laboratory, Cornell University, Ithaca, New York 14853-1301

Received May 27, 1994

1. Introduction

The reactivity of an interface is extensively determined by its composition and structure[1] so that their study can yield very valuable information not only from a fundamental scientific point of view but also from technological and economic perspectives. Of particular importance are interfacial structural and compositional changes that may arise as a result of various physicochemical perturbations such as applied potential, pH, and others since in many cases these changes will greatly influence reactivity. These investigations are relevant to the understanding of many fundamental problems such as electron transfer, adsorption, catalysis, corrosion, and the distribution of ionic species at charged surfaces, especially at solid/liquid interfaces. Of these, the electrode/solution interface is of particular relevance, and we focus our attention on it. In-situ structural and compositional studies of electrochemical interfaces are confronted by various difficulties, the principal one being the inability of many surface-sensitive structural techniques to probe a condensed phase.

Because of their penetrative power, X-rays are ideally suited for in-situ studies of interfaces in general and solid/liquid interfaces in particular. The recent advent of powerful X-ray synchrotron sources has made experiments of this type feasible. Synchrotron sources offer a broad spectral range of polarized, highly collimated X-rays with intensities that are 10^3–10^6 higher than those of conventional sources.[2] Moreover, third-generation synchrotron sources, with their projected increase in brightness on the order of 10^4, will allow for new types of experiments, including the study of dynamic processes in real time.

There are a number of X-ray-based surface-sensitive techniques that can be employed in the study of solid/liquid interfaces, including surface EXAFS,[3] X-ray standing waves (XSW),[4] grazing incidence X-ray diffraction (GIXD),[5] and others.[6]

In this Account we focus on the use of XSW and surface EXAFS. We begin with a brief theoretical description followed by experimental aspects of these techniques. We then discuss specific examples with emphasis on the underpotential deposition (UPD; see below)[7] of copper on platinum in the presence and absence of coadsorbates, the potential dependent distribution of interfacial species, and potential dependent structural changes of a redox-active self-assembling monolayer.

H. D. Abruña was born in Santurce, Puerto Rico, in 1953. Through high school, he was educated on the Island. He obtained B.S. and M.S. degrees in chemistry from Rensselaer Polytechnic Institute in 1975 and 1976, respectively, and a Ph.D. (1980) in analytical chemistry from the University of North Carolina at Chapel Hill under Profs. R. W. Murray and T. J. Meyer. From July 1980 through December 1981 he was a postdoctoral associate under Prof. A. J. Bard. After a brief (1982–1983) stay in the Chemistry Department of the University of Puerto Rico, he went to Cornell in 1983, where he is currently Emile M. Chamot Professor of Chemistry. He is an avid runner and a prodigious consumer of espresso.

G. M. Bommarito was born in Milano, Italy (1962), and came to the United States in 1975. He obtained a B.S. in physics from Loyola (Chicago) in 1984, an M.S. in applied physics from Cornell in 1987, and a Ph.D. in chemistry from Cornell in 1992. After a postdoctoral fellowship with P. Pershan at Harvard, he joined 3M in 1994.

H. S. Yee was born in Boston in 1964. He obtained a B.S. in chemistry from Brown in 1987, an M.S. in environmental engineering from Caltech in 1989, and a Ph.D. in chemistry from Cornell in 1994. He is currently involved in defense and technology policy with the RAND Corporation.

2. Brief Theoretical Description

A. X-ray Standing Waves. The X-ray standing wave technique is a sensitive tool for determining the position of atoms within a crystal, adsorbed onto a surface, or distributed within the crystal or at the interface. The technique is based on the X-ray standing wave field (of period $D = \lambda/2 \sin \theta$; where λ is the wavelength of the traveling waves and 2θ is the relative angle between them) that arises as a result of the interference between coherently related incident and reflected plane waves and is described by the theory of dynamical diffraction of X-rays.[8] Standing waves can be generated by either Bragg diffraction or total external reflection.

Conventional XSW are generated using dynamical Bragg diffraction[4,8,9] from perfect single crystals. The periodicity of the standing wave field is equivalent to the d-spacing of the (hkl) diffracting planes, making

† G. M. Bommarito, 3M Adhesive Tech. Center, 3M Center, Building 236-GA-03, St. Paul, MN 55144-1000.

‡ H. S. Yee, RAND Corp., 1700 Main St., Santa Monica, CA 90407.

(1) (a) Adamson, A. W. *Physical Chemistry of Surfaces*; Wiley: New York, 1982. (b) Somorjai, G. A. *Chemistry in Two Dimensions: Surfaces*, Cornell University Press: Ithaca, 1981. (c) Somorjai, G. A. *Introduction to Surface Chemistry and Catalysis*; Wiley: New York, 1994. (d) Israelachvili, J. N. *Intermolecular and Surface Forces*; Academic Press: London, 1985.

(2) Winick, H., Doniach, S., Eds. *Synchrotron Radiation Research*; Plenum: New York, 1980.

(3) (a) Citrin, P. H. *J. Phys., Colloq.* **1986**, No. C8, *47*, 437. (b) Lee, P. A.; Citrin, P. H.; Eisenberger, P.; Kincaid, B. M. *Rev. Mod. Phys.* **1981**, *53*, 769. (c) Teo, B. K. *EXAFS: Basic Principles and Data Analysis*; Springer-Verlag: Berlin, 1986. (d) Koningsberger, D. C., Prins, R., Eds. *X-Ray Absorption: Principles, Applications, Techniques of EXAFS, SEXAFS, and XANES*; John Wiley & Sons: New York, 1988.

(4) Batterman, B. W. *Phys. Rev.* **1964**, *133*, A759.

(5) (a) Marra, W. C.; Eisenberger, P.; Cho, A. Y. *J. Appl. Phys.* **1979**, *50*, 6927. (b) Eisenberger, P.; Marra, W. C. *Phys. Rev. Lett.* **1981**, *46*, 1081. (c) Marra, W. C.; Fuoss, P. H.; Eisenberger, P. E. *Phys. Rev. Lett.* **1982**, *49*, 1169.

(6) See: Abruña, H. D., Ed. *Electrochemical Interfaces*; VCH Publishers: Boca Raton, 1992.

(7) (a) Kolb, D. M. In *Advances in Electrochemistry and Electrochemical Engineering*; Gerisher, H., Tobias, C., Eds.; J. Wiley and Sons: New York, 1978; Vol. 11. (b) Adzic, R. *Isr. J. Chem.* **1979**, *18*, 166. (c) Adzic, R. In *Advances in Electrochemistry and Electrochemical Engineering*; Gerisher, H., Tobias, C., Eds.; J. Wiley and Sons: New York, 1985, Vol. 13. (d) Juttner, K.; Lorenz, W. J. *Z. Phys. Chem.* **1980**, *122*, 163. (e) Lorenz, W. J.; Hermann, H. D.; Wuthrich, N.; Hilbert, F. *J. Electrochem. Soc.* **1974**, *121*, 1167. (f) Szabo, S. *Int. Rev. Phys. Chem.* **1991**, *10*, 207.

(8) von Laue, M. *Roentgenstrahlinterenzen*; Akademische Verlagsgesellschaft: Frankfurt, 1960. For a review, see: Batterman, B. W.; Cole, H. *Rev. Mod. Phys.* **1964**, *36*, 681.

0001-4842/95/0128-0273$09.00/0

this technique a very precise tool (±1% of the d-spacing)[9b] for measuring bond lengths between adsorbate atoms and surface/bulk lattice positions over the range 1−4 Å (i.e., typical d-spacings for single crystals). Long-period XSW, appropriate for measurements over long length scales, can be generated by Bragg diffraction from layered synthetic microstructures[10,11] (LSMs) which have d-spacings ranging from 20 to 200 Å or by employing total external reflection from a mirror surface.[12]

For XSW based on Bragg reflection, the nodal and antinodal planes of the standing wave are parallel to and the nodal wavelength is equivalent to those of the diffracting planes. As the angle of incidence is advanced across the Bragg reflection, the standing wave field moves in the $-H$ direction (that is, toward the surface) normal to the diffraction planes by $^1/_2$ of a d-spacing. Thus, the standing wave can be made to sample an adsorbate or overlayer at varying positions above the substrate interface.

Using an incident X-ray beam energy at or beyond the absorption edge of the atoms in the overlayer, the fluorescence emission yield will be modulated as the incident angle is advanced across the Bragg reflection. The yield can be expressed as an integral that incorporates a distribution function $F(z)$ for the atoms in the adlayer:

$$Y(\theta) = \int I(z,\theta)\, F(z)\, \mathrm{d}z \qquad (1)$$

The phase and amplitude of this modulation (or so-called coherent position and coherent fraction) are a measure of the mean position $\langle z \rangle$ and width $\sqrt{\langle z \rangle^2}$, respectively, of the distribution, $F(z)$, of atoms in the overlayer. The coherent fraction can vary from 0 to 1 corresponding to the limiting cases of random and completely coherent distributions. In the case of a random distribution (i.e., zero coherent fraction), the yield will be given by $1 + R$, where R is the reflectivity. In the case of length scales of tens of angstroms (e.g., ionic distributions at charged surfaces), it is best to employ Bragg diffraction from LSMs[10−11] with d-spacings from about 20 to 200 Å or XSW based on total external reflection from a mirror surface.[12] XSW have been used in a number of studies of electrochemical as well as other solid/liquid interfaces.[13−15]

(9) (a) Materlik, G.; Frahm, A.; Bedzyk, M. J. *Phys. Rev. Lett.* **1984**, *52*, 441. (b) Bedzyk, M. J.; Materlik, G. *Phys. Rev. B*, **1985**, *31*, 4110. (c) Cowan, P. L.; Golovchenko, J. A.; Robbins, M. F. *Phys. Rev. Lett.* **1980**, *44*, 1680. (d) Zegenhagen, J.; Huang, K.-G.; Gibson, W. M.; Hunt, B. D.; Schowalter, L. J. *Phys. Rev. B* **1989**, *39*, 10254.

(10) Underwood, J. H.; Barbee, T. W. *AIP Conf. Proc.* **1981**, No. 75, 170.

(11) (a) Barbee, T. W.; Underwood, J. H. *Opt. Commun.* **1983**, *48*, 161. (b) Barbee, T. W.; Warburton, W. K. *Mater. Lett.* **1984**, *3*, 17.

(12) Bedzyk, M. J.; Bommarito, G. M.; Schildkraut, J. S. *Phys. Rev. Lett.* **1989**, *62*, 1376.

(13) (a) Materlik, G.; Zegenhagen, J.; Uelhoff, W. *Phys. Rev. B* **1985**, *32*, 5502. (b) Materlik, G.; Schmah, M.; Zegenhagen, J.; Uelhoff, W. *Ber. Bunsen-Ges. Phys. Chem.* **1987**, *91*, 292. (c) Zegenhagen, J.; Materlik, G.; Uelhoff, W. *J. X-ray Sci. Technol.* **1990**, *2*, 214.

(14) (a) Bedzyk, M. J.; Bilderback, D.; White, J. H.; Abruña, H. D.; Bommarito, G. M. *J. Phys. Chem.* **1986**, *90*, 4926. (b) Bommarito, G. M.; White, J. H.; Abruña, H. D. *J. Phys. Chem.* **1990**, *94*, 8280. (c) Abruña, H. D.; Bommarito, G. M.; Acevedo, D. *Science* **1990**, *250*, 69. (d) Bommarito, G. M.; Acevedo, D.; Rodríguez, J. F.; Abruña, H. D. In *X Rays in Materials Analysis II: Novel Applications and Recent Developments*; Mills, D. M., Ed.; SPIE Proceedings Vol. 1550; SPIE: Bellingham, WA, 1991; pp 156−170. (e) Abruña, H. D.; Gog, T.; Materlik, G.; Uelhoff, W. *J. Electroanal. Chem.* **1993**, *360*, 315.

(15) (a) Bedzyk, M. J.; Bilderback, D. H.; Bommarito, G. M.; Caffrey, M.; Schildkraut, J. S. *Science* **1988**, *241*, 1788. (b) Bedzyk, M. J.; Bommarito, G. M.; Caffrey, M.; Penner, T. L. *Science* **1990**, *248*, 52.

B. Surface EXAFS. EXAFS refers to the modulations in the X-ray absorption coefficient beyond an absorption edge and involves the measurement of the absorption coefficient (or any parameter that can be related to it) as a function of photon energy.[3] These modulations arise as a result of the interference between the outgoing wave (due to the photoionization of a core-level electron upon absorption of an X-ray photon) and a backscattered wave due to the presence of near neighbors (typically at 5 Å or closer; EXAFS is only sensitive to short-range order). The modulations present at energies from about 40 eV to 1000 eV beyond the edge are termed EXAFS. To a good approximation, the frequency of the EXAFS oscillations will depend on the distance between the absorber and its near neighbors, whereas the amplitude will depend on the numbers and types of neighbors as well as their distance from the absorber. From an analysis of the EXAFS one can obtain information on near neighbor distances (to ±0.02 Å), numbers (to ±20%), and types. Further advantages of EXAFS are that it can be applied to all forms of matter, that for solid samples single crystals are not required, and that, by choosing the X-ray energy, one can focus on the environment around a particular element. Furthermore, the energetic location of the absorption edge can be used to determine the effective oxidation state of the absorbing atom.

In the region close to the absorption edge (generally termed XANES: X-ray absorption near edge structure), the spectrum is very rich in structural information. However, the theoretical modeling is quite complex due to multiple scattering effects, although there have been recent theoretical advances in the analysis.[18]

Surface EXAFS offers an additional experimental handle, and this refers to the polarization dependence of the signal since only those bonds whose interatomic vector has a projection in the plane of polarization of the incident beam will contribute to the observed EXAFS. Thus, polarization dependence studies can provide a wealth of information concerning adsorption sites and near neighbor geometries.

Surface EXAFS has been applied to the study of a number of electrochemical systems,[19,20] with emphasis on electrodeposition of metal monolayers.

3. Experimental Aspects

Surface EXAFS and X-ray standing wave measurements are, in general, experimentally demanding. Of particular importance is the alignment of the sample relative to the beam. An XSW experiment typically consists of monitoring some signal proportional to the standing wave electric field intensity (such as characteristic fluorescence) as the angle of incidence is scanned across a Bragg reflection or through the total external reflection. A typical experimental setup consists of (1) a collimated beam whose intensity, I_0, is monitored with an ion chamber; (2) a sample stage;

(16) (a) Teo, B. K.; Lee, P. *J. Am. Chem. Soc.* **1979**, *101*, 2815. (b) McKale, A. G.; Veal, B. W.; Paulikas, A. P.; Chan, S.-K.; Knapp, G. S. *J. Am. Chem. Soc.* **1988**, *110*, 3763.

(17) Citrin, P. H.; Eisenberger, P.; Kincaid, B. M. *Phys. Rev. Lett.* **1976**, *36*, 1346.

(18) (a) Rehr, J. J.; Albers, R. C.; Natoli, C. R.; Stern, E. A. *Phys. Rev. B* **1986**, *34*, 4350. (b) Mustre de Leon, J.; Rehr, J. J. *J. Phys. B* **1989**, *158*, 543. (c) Mustre de Leon, J.; Rehr, J. J.; Natoli, C. R.; Fadley, C. S. *Phys. Rev. B* **1990**, *41*, 8139.

(3) a reflected beam monitor, I_R; and (4) a fluorescence detector at 90° relative to the incident X-ray beam. The angular resolution of the sample stage is especially important since a typical reflection width for a single crystal will be on the order of tens of microradians and a few milliradians for LSMs. At each angular position, a complete X-ray fluorescence spectrum is collected and later analyzed so as to accurately determine the fluorescence yield.

A similar experimental setup is employed in the case of surface EXAFS experiments except that in this case the sample is fixed relative to the beam, the incident beam energy is scanned across an absorption edge of the material under study, and the fluorescence intensity is monitored as a function of incident energy.

In addition, the design of the cell requires careful consideration so that it fulfills the requirements imposed by both the X-ray and electrochemical aspects of the experiment.

Analysis of X-ray standing wave data is based on a fit of the data (reflectivity and fluorescence yield) to those predicted from theory.[21] In the case of surface EXAFS, the basic aim is to be able to extract information related to interatomic distances, numbers, and types of backscattering neighbors. Details on data analysis are beyond the scope of this Account, and the interested reader is referred to the pertinent literature.[3]

4. Examples

We will consider three studies: (A) mechanism of copper UPD on an iodine-covered surface; (B) surface EXAFS of Cu UPD on Pt(111) in the presence and absence of chloride; and (C) potential dependent structural changes of a redox-active self-assembling monolayer.

A. Mechanism of Copper UPD on an Iodine-Covered Surface. We have carried out a study of the mechanism of copper underpotential deposition (UPD) on an iodine-covered platinum surface.[14d,21b,22,23] UPD refers to the electrodeposition of metal monolayer(s) at potentials positive of the reversible Nernst value and provides one of the most precise means of controlling coverages from submonolayer to monolayer and in some cases multilayer coverages in a quantifiable and reproducible fashion.[7] We employed a Pt/C LSM as both the electrode and the diffracting structure and an X-ray energy of 9.35 keV, just above the K absorption edge for copper. From voltammetry in sulfuric acid we have previously established that the Pt surface of the LSM is (111), in character with randomly distributed monatomic steps.[14b,24] From fits to the Bragg and specular reflectivity measurements we determined the interfacial roughness to be 6.8 ± 0.5 Å, which correlated very well with that calculated for a Pt(111) surface with randomly distributed monatomic steps (6.28 Å), consistent with the voltammetric results previously mentioned.

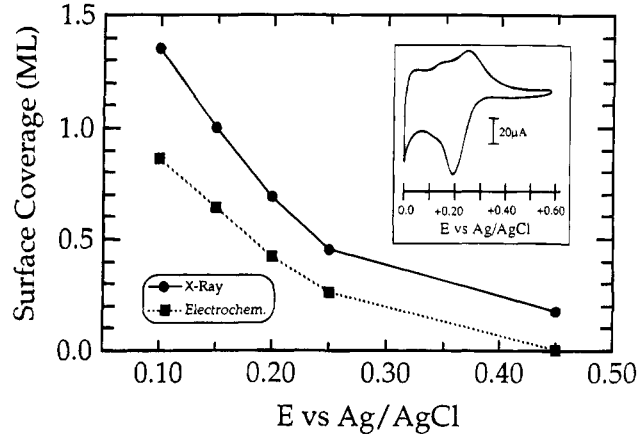

Figure 1. X-ray and electrochemical derived surface coverages for copper as a function of applied potential. Inset: Cyclic voltammogram for copper deposition on an iodine-coated Pt/C LSM at 20 mV/s in a solution containing 0.63 mM Cu^{2+} and 0.1 M H_2SO_4.

We carried out measurements at applied potentials of +0.45, +0.25, +0.20, +0.15, and +0.10 V corresponding to surface coverages of approximately 0, 1/4, 1/2, 3/4, and 1 monolayer of copper, respectively. Surface coverages were determined from both electrochemical (by integration of the area under the voltammetric wave; see inset to Figure 1 for cyclic voltammogram) and X-ray fluorescence measurements. Upon comparison (Figure 1), we find that there appears to be a considerable amount of copper which is electrochemically inactive and whose concentration is potential dependent. In fact, even at potentials where there is no evidence of electrodeposited copper (+0.45 V) the X-ray fluorescence data indicate the presence of approximately 20% of a monolayer. Such copper species would appear to form what could be termed a "preadsorbed" state. This copper layer is weakly associated with the electrode surface as it is easily removed upon rinsing with supporting electrolyte. We do not believe that this interaction is due to electrostatic effects since at +0.45 V the electrode is positive relative to the solution (i.e., we are positive of the potential of zero charge, E_{PZC}) and, in addition, all charge screening would be by the supporting electrolyte, which is in very large excess (over 100-fold) relative to the copper ions present in solution. Thus we ascribe the presence of this copper layer to a specific interaction with the iodine adlayer on the

(19) (a) Blum, L.; Abruña, H. D.; White, J. H.; Gordon, J. G., II; Borges, G. L.; Samant, M. G.; Melroy, O. R. *J. Chem. Phys.* **1986**, *85*, 6732. (b) Melroy, O. R.; Samant, M. G.; Borges, G. L.; Gordon, J. G., II; Blum, L.; White, J. H.; Albarelli, M. J.; McMillan, M.; Abruña, H. D. *Langmuir* **1988**, *4*, 728. (c) White, J. H.; Albarelli, M. J.; Abruña, H. D.; Blum, L.; Melroy, O. R.; Samant, M. G.; Borges, G. L.; Gordon, J. G., II. *J. Phys. Chem.* **1988**, *92*, 4432. (d) Abruña, H. D.; White, J. H.; Albarelli, M. J.; Bommarito, G. M.; Bedzyk, M. J.; McMillan, M. J. *J. Phys. Chem.* **1988**, *92*, 7045. (e) White, J. H.; Abruña, H. D. *J. Phys. Chem.* **1988**, *92*, 7131. (f) White, J. H.; Abruña, H. D. *J. Electroanal. Chem.* **1989**, *274*, 185. (g) Abruña, H. D. In *Advances in Chemical Physics*; Prigogine, I., Rice, S. A., Eds.; John Wiley & Sons, Inc.: New York, 1990; Vol. 77, Chapter 5, pp 255–335.

(20) (a) Samant, M. G.; Borges, G. L.; Gordon, J. G.; Melroy, O. R.; Blum, L. *J. Am. Chem. Soc.* **1987**, *109*, 5970. (b) Tourillon, G.; Guay, D.; Tadjeddine, A. J. *Electroanal. Chem.* **1990**, *289*, 263. (c) Tadjeddine, A. J.; Guay, D.; Ladouceur, M.; Tourillon, G. *Phys. Rev. Lett.* **1991**, *66*, 2235. (d) Furtak, T. E.; Wang, L.; Creek, E. A.; Samamta, P.; Hayes, T. M.; Kendall, G.; Li, W.; Liang, G.; Lo, C.-M. *Electrochim. Acta* **1991**, *36*, 1869. (e) McBreen, J.; O'Grady, W. E.; Tourillon, G.; Dartyge, E.; Fontaine, A. *J. Electroanal. Chem.* **1991**, *307*, 229. (f) Durand, R.; Faure, R.; Aberdam, D.; Salem, C.; Tourillon, G.; Guay, D.; Ladoceur, M. *Electrochim. Acta* **1992**, *37*, 1977.

(21) (a) Parratt, L. G. *Phys. Rev.* **1954**, *95*, 359. (b) Bommarito, G. M. Ph.D. Thesis, Cornell University, 1992.

(22) Bommarito, G. M.; Acevedo, D.; Rodríguez, J. F.; Abruña, H. D. *J. Electroanal. Chem.* **1994**, *379*, 135.

(23) (a) Stickney, J. L.; Rosasco, S. D.; Song, D.; Soriaga, M. P.; Hubbard, A. T. *Surf. Sci.* **1983**, *130*, 326. (b) Hubbard, A. T.; Stickney, J. L.; Rosasco, S. D.; Soriaga, M. P.; Song, D. *J. Electroanal. Chem.* **1983**, *150*, 165. (c) Stickney, J. L.; Rosasco, S. D.; Hubbard, A. T. *J. Electrochem. Soc.* **1984**, *131*, 260.

(24) Aberdam, D.; Durand, R.; Faure, R.; El-Omar, F. *Surf. Sci.* **1986**, *171*, 303.

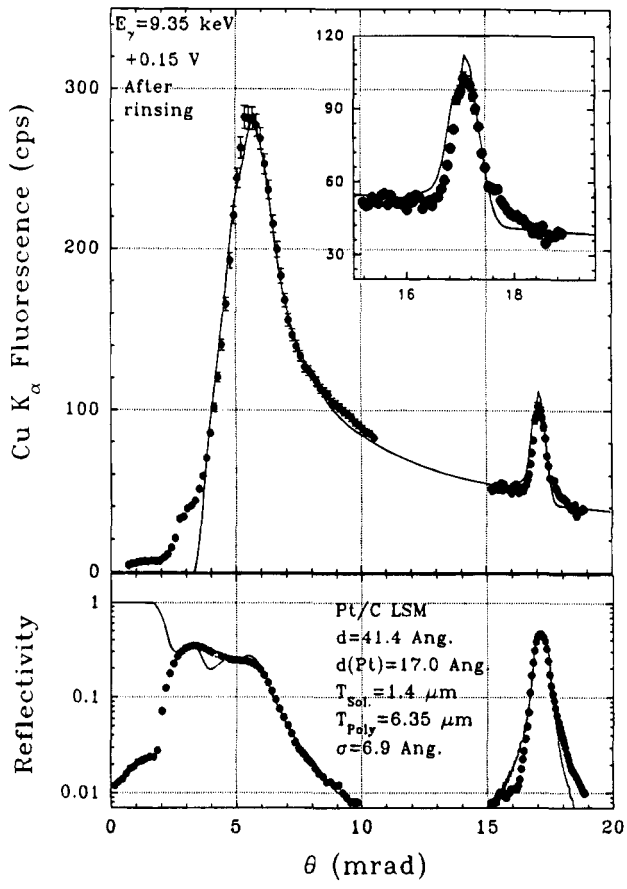

Figure 2. Top panel: The XSW fluorescence profiles for both total external reflection and Bragg diffraction regimes at +0.15 V after rinsing of the electrode surface with clean electrolyte. A magnified view of the Bragg data is show in the inset. Bottom panel: Complete reflectivity profile. In both cases fits to the data were performed over the entire angular range simultaneously and are plotted as solid lines.

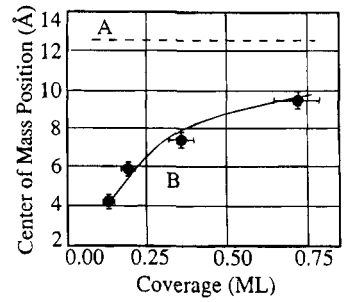

Figure 3. Variation of the center of mass in the copper adlayer as a function of surface coverage. Curve A represents the expected variation in the center of mass for a model in which filling of the surface sites is random, whereas B represents the variation expected for a model where the surface sites are filled sequentially starting with the deepest ones first. Points are experimental data.

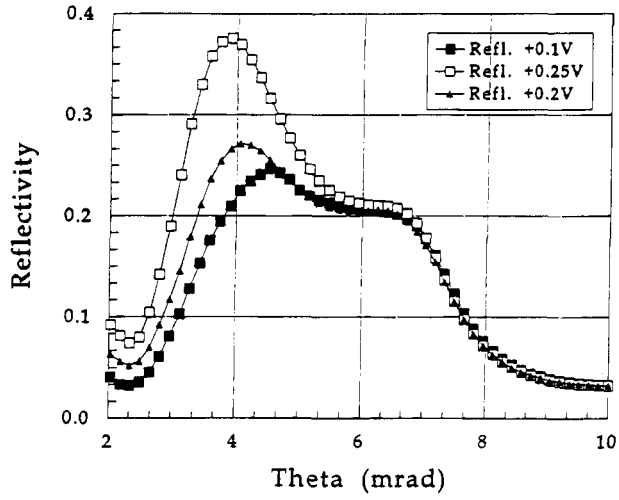

Figure 4. Reflectivity profiles (at 9.35 keV) as a function of applied potential for an iodine-coated Pt/C LSM in contact with a 0.1 M H_2SO_4 solution containing 0.63 mM Cu^{2+}.

platinum surface. These are important observations in that they imply that there can be very significant differences in bulk and interfacial concentrations of reactants (which are not due to electrostatic attraction/repulsion) at potentials where no redox reactions are taking place.

We have also measured the standing wave profiles for both total external reflection and Bragg diffraction after deposition at potentials of +0.25, +0.20, +0.15, and +0.10 V and after rinsing the electrode with clean supporting electrolyte (no copper present in solution) while maintaining potential control over the system at all times. Data over both angular regimes were analyzed simultaneously, allowing us to probe the same distribution of species on two rather different length scales and two different z-scale (normal to the electrode surface) origins, leading to an unambiguous result. The best theoretical fits are shown as solid lines in Figure 2 for an applied potential of +0.15 V. In addition, the bottom panel shows the reflectivity profiles and corresponding fits.

From XSW data one can obtain information on the distribution profile of interfacial species. In this case the interest was in the potential dependence of such a distribution. A particularly useful way of presenting the data was to plot the center of mass (i.e., the z-position where 50% of the total amount of copper is reached) of each distribution as a function of coverage since it can provide valuable insights into the mechanism of deposition since the center of mass depends on both the peak position and the width (fwhm) of a given distribution. We considered two models that represented limiting cases. In the first, if surface sites were occupied in a random mode, one would expect a homogeneous copper distribution whose center of mass was always at the same z-position, namely, the center of the Gaussian representing the surface site concentration profile. Alternatively, one could have a model in which surface sites are occupied sequentially with the deepest ones first. In this case, the center of mass position would vary with the copper surface coverage. Both of these models are plotted, along with the experimental data, in Figure 3 as a function of coverage, with the dashed line representing the former and the solid line the latter. The points represent experimental values. It is immediately clear that the observed results are in excellent agreement with the model that involves sequential filling of available surface sites with the deepest ones being occupied first. This finding implies that the more favorable surface sites for deposition are the ones closest to the platinum bulk lattice, either because the substrate–deposit interactions are maximized at these sites (due to higher local coordination) or because the interaction with the electric fields present at the interface is greatest at these locations. In addition, either the deposited copper atoms diffuse to these positions or

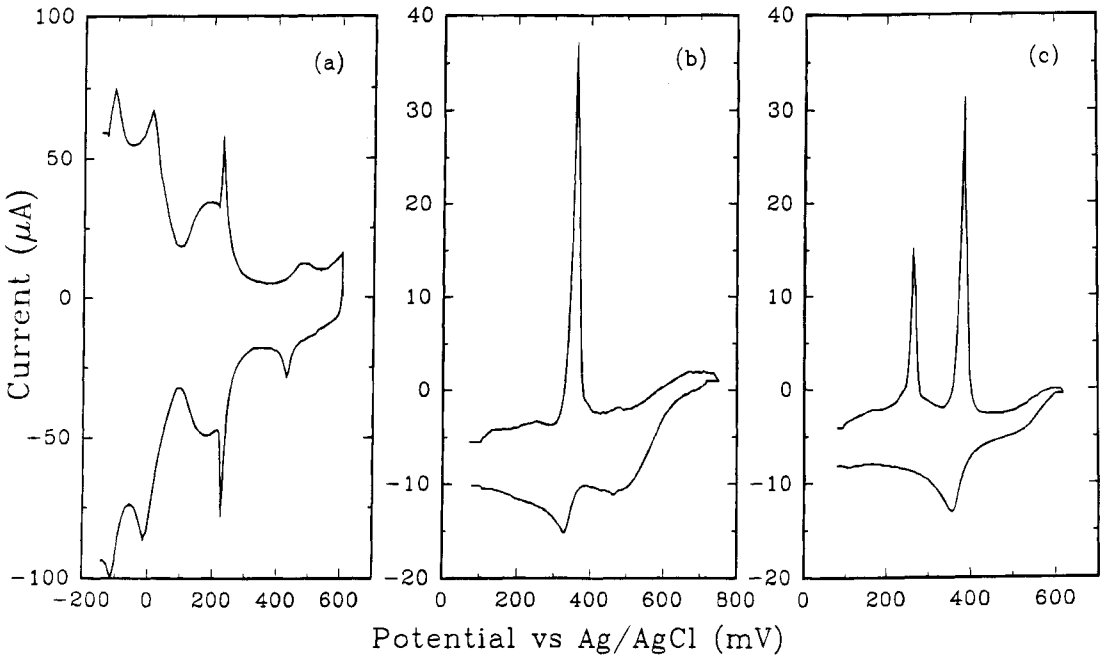

Figure 5. Cyclic voltammograms inside X-ray absorption spectroscopy cell for a Pt(111) electrode in the presence of (a) a 0.1 M H_2SO_4 solution (sweep rate, 50 mV/s); (b) a 0.1 M H_2SO_4 solution containing 50 μM copper (sweep rate, 2 mV/s); and (c) a 0.1 M H_2SO_4 solution containing 50 μM copper and 1 mM Cl^- (sweep rate, 2 mV/s).

the deposition process itself is enhanced or catalyzed by these particular sites.

We have also carried out reflectivity measurements which yield the electron density profile in a direction normal to the surface and can be used to determine surface roughness (as discussed previously) as well as the distribution of interfacial species in a direction normal to the surface.

In the studies mentioned above, there was a peak in the reflectivity profile at 3.0 mrad with a critical angle of 3.5 mrad (see bottom panel of Figure 2). This was a surprising observation since, for a solution layer of the supporting electrolyte used (0.63 mM Cu sulfate in 0.10 M H_2SO_4) with a uniform electron density distribution, the critical angle is expected to be 2.3 mrad. If one assumes that this unexpected reflectivity peak is due to total external reflection from the solution layer, this implies that the electron density distribution is nonuniform. In addition, the intensity and angular position of this reflectivity peak were potential dependent (Figure 4), implying that there is a potential-driven rearrangement of this distribution. These findings are most notable in that they indicate that it might be possible to measure directly potential dependent interfacial ionic gradients. From a preliminary analysis of these data we find that these potential dependent variations are generally in good agreement with predictions from simple models of the double layer.

B. Surface EXAFS Study of Cu UPD on Pt(111) in Sulfate Media and in the Presence of Chloride Anions. We have carried out in-situ surface EXAFS studies of the potential dependent changes of the copper UPD layer on a clean and well-ordered Pt(111) surface in sulfuric acid in the absence[25] and presence[26] of chloride ions. The first point of note is that we were able to develop a protocol for electrode pretreatment so that the electrochemical response *in the X-ray cell* was identical to that obtained in a conventional electrochemical cell. This is depicted in Figure 5a, which shows the "butterfly" pattern characteristic of a clean and well-ordered Pt(111) electrode.[27] In addition the voltammetries for copper UPD on Pt(111) in the absence (Figure 5b) and presence of chloride (Figure 5c) are also very sharp, with the characteristic double peak seen in the latter.[28]

As mentioned above, we carried out studies in the presence and absence of chloride. In the absence of chloride, XANES and EXAFS analyses were made as a function of applied potential (+0.20, +0.10, and 0.0 V) corresponding to coverages of approximately 0.50, 0.75, and 1.0 ML, respectively. Spectra in the presence and absence of chloride at an applied potential of +0.10 V are presented in Figure 6.

From the charge derived from electrochemical measurements it appears that, at the three potentials studied in the absence of chloride, the electrodeposited copper was not completely discharged. The XANES analysis (see inset to Figure 6a for data at +0.10 V) revealed similarities between the copper adlayer and the Cu_2O reference lending support to earlier findings[19e,28,29] of a partially discharged copper adlayer. Oxygen is a persistent backscatterer, and the Cu–O distance remained relatively unchanged at all potentials studied. In the σ-polarization (in-plane) we observed intense copper–copper scattering at all potentials studied.

At 0.0 V we find the copper–copper distance to be 2.77 ± 0.03 Å with a coordination number of 6.3 ± 20%. At this potential the copper adlattice exhibits an epitaxial arrangement with the Pt(111) surface. At +0.10 V the copper–copper bond distance is 2.85 ±

(25) Yee, H. S.; Abruña, H. D. *J. Phys. Chem.* **1993**, *97*, 6278.
(26) Yee, H. S.; Abruña, H. D. *Langmuir* **1993**, *9*, 2460.
(27) Clavillier, J. *J. Electroanal. Chem.* **1980**, *107*, 211.
(28) (a) White, J. H.; Abruña, H. D. *J. Phys. Chem.* **1990**, *94*, 894. (b) Kolb, D. M.; Al Jaaf-Golze, K.; Zei, M. S. *DECHEMA-Monographien Bd. 102*; VCH: Weinheim, 1986.
(29) (a) Leung, L.-W. H.; Gregg, T. W.; Goodman, D. W. *Langmuir* **1991**, *7*, 3205. (b) Leung, L.-W. H.; Gregg, T. W.; Goodman, D. W. *Chem. Phys. Lett.* **1992**, *188*, 467.

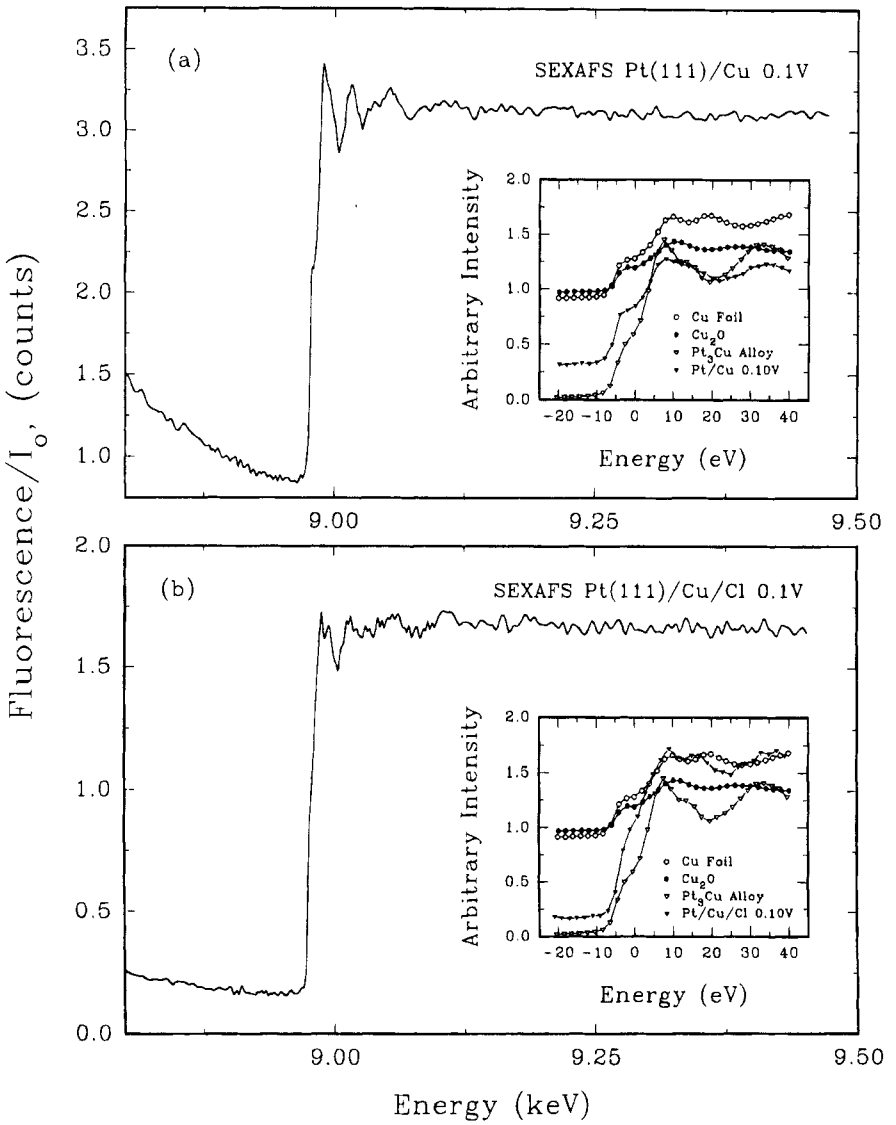

Figure 6. In-situ surface EXAFS spectra around the Cu K edge for copper underpotentially deposited on a Pt(111) electrode surface at 0.10 V (vs Ag/AgCl) and in the absence (a) and presence (b) of 1 mM Cl^-. Insets: Near edge regions and comparison with model compounds.

0.03 Å. Here the copper adlayer has expanded, which is to be expected for a lower coverage. At 0.0 and +0.10 V we see the formation of well-ordered hexagonal surface structures. At +0.20 V, where the coverage is about 0.5 ML, we find that there are two copper–copper distances of 2.66 ± 0.03 and 2.87 ± 0.03 Å with coordination numbers of 6.2 ● 20% and 5.7 ± 20%, respectively. This suggests the formation of two clusters with a hexagonal structure.

As mentioned above, the copper–copper distance was found to be strongly dependent on the coverage, whereas the copper–oxygen bond distance was not. From analysis of our data, consideration of possible adsorption sites, and comparison of our results with the predictions from the recently published model of Reher and co-workers,[18] the copper adatoms appear to occupy 3-fold hollow sites on the platinum surface.[30]

In the presence of chloride we observe a contraction in the copper adlattice (relative to the value in the absence of chloride) for a comparable amount of deposited copper. At an applied potential of +0.10 V, the Cu–Cu bond distance was found to be 2.59 ± 0.03 Å in comparison to 2.85 ± 0.03 Å (in the absence of chloride), with the former being very close to the bulk value for copper (2.56 Å) and suggesting a much smaller residual charge on the copper. In addition, the near edge features (see inset to Figure 6b) are also consistent with this. Moreover, there is no evidence for oxygen backscattering. The chloride appears to play a significant role in ordering the copper adlayer. At full monolayer coverage of copper, there is no in-plane scattering attributable to chloride, suggesting that the chloride forms an adlayer over the electrodeposited copper (on a-top sites) and serves as a "protective" overlayer precluding oxygen adsorption.

C. Potential Dependent Structural Changes of a Redox-Active Self-Assembling Monolayer. We have carried out an XSW study on a redox-active self-assembling monolayer. The system studied was the osmium complex $[Os(bpy)_2(dpyp)Cl]^+$ (bpy is 2,2′-bipyridine, and dpyp is 1,3-di(4-pyridyl)propane), whose structure is presented in Figure 7A. This material and related complexes[31–33] adsorb very strongly to platinum electrodes, and the surface-immobilized

(30) Yee, H. S.; Abruña, H. D. *J. Phys. Chem.* **1994**, *98*, 6552.

(31) Acevedo, D.; Abruña, H. D. *J. Phys. Chem.* **1991**, *95*, 9590.

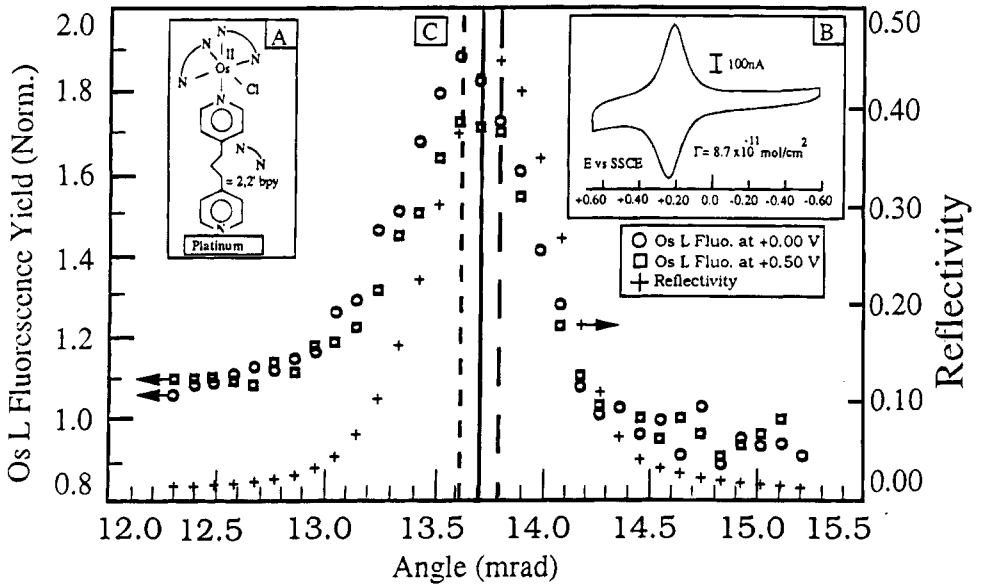

Figure 7. (A) Structure of self-assembling, redox-active osmium complex. (B) Cyclic voltammetric response for the osmium complex adsorbed on a platinum electrode. (C) Reflectivity profile and angular dependence of the Os_L fluorescence intensity at 0.00 and +0.50 V for a Pt/C LSM coated with a monolayer of the osmium complex (adapted from ref 14c).

complex exhibits a very well-behaved electrochemical response (Figure 7B). A saturation coverage representing a compact monolayer (1 ML represents about 1×10^{-10} mol/cm^2) is achieved for solution concentrations above 4 μM.

We employed a Pt/C LSM as the electrode and modified it with a monolayer of the complex. An incident X-ray beam energy of 11.1 keV was employed to excite Os_L fluorescence. In all cases a reflectivity profile was collected simultaneously with the Os_L fluorescence intensity. Experiments were carried out at applied potentials of 0.0 and +0.50 V where the osmium center within the complex is present as Os(II) and Os(III), respectively. It should be noted that the overall charge on the complex changes from +1 to +2 upon electrochemical oxidation.

Data for the Os_L fluorescence intensity at 0.0 and +0.50 V as well as a reflectivity profile are presented in Figure 7C. We focus, specifically, on the angular position of the fluorescence maxima and on the width of the fuorescence profile. As can be seen in Figure 7C, the maximum in the fluorescence at 0.0 V occurs at a lower angle than at +0.50 V. In addition, the fluorescence intensity is lower and the distribution broader at +0.50 V relative to the values at 0.0 V. There are some qualitative observations that may be made. The fact that upon oxidation at 0.50 V the fluorescence maximum shifts to a higher angle suggests that, on average, the osmium centers are closer to the electrode surface than at 0.0 V. It is worth mentioning that the distance between the osmium center and the electrode surface would be 12 Å for a fully extended chain.

The fact that the fluorescence yield profile is wider at +0.50 relative to 0.0 V would suggest that there is a broader distribution of distances. This might be due to increased coulombic repulsion between adjacent molecules since upon oxidation the charge on each molecule increases from +1 to +2. Thus, the coulombic repulsion is expected to be approximately four times as large and, in order to minimize the repulsive forces, the molecules may adopt a broader distribution in terms of distance. Moreover, additional electrochemical evidence, especially the width of the voltammetric wave as a function of coverage, is also consistent with the interpretation given above. Given the current interest in redox-active self-assembling systems, the use of XSW may provide valuable insights on potential dependent structural changes.

5. Conclusions and Future Directions

The use of X-ray-based techniques such as X-ray standing waves and surface EXAFS has yielded valuable insights on potential dependent interfacial structure and composition at electrochemical interfaces. Future applications of these techniques, especially in combination with others such as surface diffraction, will yield extremely important and fundamental information that will impact not only our understanding and control of interfacial reactivity within an electrochemical context but also other solid/liquid interfaces and the field of surface chemistry as a whole. Moreover, the advent of third-generation synchrotron sources may allow for the dynamic study of phenomena in real time.

This work was supported by the Office of Naval Research, the Materials Science Center at Cornell University, the National Science Foundation, and the Army Research Office.

AR9400296

(32) Acevedo, D.; Bretz, R. L.; Tirado, J. D.; Abruña, H. D. *Langmuir* **1994**, *10*, 1300.

(33) Tirado, J. D.; Acevedo, D.; Bretz, R. L. Abruña, H. D. *Langmuir* **1994**, *10*, 1971.